Developmental Cell
Article

# Annexin A2-Dependent Polymerization of Actin Mediates Endosome Biogenesis

Etienne Morel,[1,3] Robert G. Parton,[2] and Jean Gruenberg[1,*]
[1]Department of Biochemistry, University of Geneva, 30 Quai E. Ansermet, 1211 Geneva 4, Switzerland
[2]Institute for Molecular Bioscience and Center for Microscopy and Microanalysis, University of Queensland, Brisbane 4072, Australia
[3]Present address: Department of Pathology and Cell Biology, Taub Institute, Columbia University Medical Center, New York, NY 10032, USA
*Correspondence: jean.gruenberg@biochem.unige.ch
DOI 10.1016/j.devcel.2009.01.007

## SUMMARY

**Early endosomes give rise to multivesicular intermediates during transport toward late endosomes. Much progress has been made in understanding the sorting of receptors into these intermediates, but the mechanisms responsible for their biogenesis remain unclear. Here, we report that F-actin is necessary for transport beyond early endosomes and endosome formation. We found that endosomes captured by actin cables were essentially stationary, but early endosomes also exhibited patches of F-actin and facilitated selective F-actin nucleation and polymerization. Our data show that nucleation of actin patches by early endosomes is strictly dependent on annexin A2, a protein involved in early-to-late endosome transport. It also requires the actin nucleation factor Spire1 and involves Arp2/3, which is needed for filament branching. We conclude that actin patches are nucleated on early endosomes via annexin A2 and Spire1, and that these patches control endosome biogenesis, presumably by driving the membrane remodeling process.**

## INTRODUCTION

Cell surface proteins and lipids, as well as solutes and ligands, can be internalized into animal cells by several pathways, which converge in a common early endosome, where they are sorted to various cellular destinations (Gruenberg, 2001; Mayor and Pagano, 2007). Some molecules, e.g., housekeeping receptors, are recycled to the plasma membrane directly or indirectly via recycling endosomes, or transported to the trans-Golgi network, whereas others, particularly downregulated signaling receptors, are targeted to late endosomes and lysosomes to be degraded. These receptors are sorted into invaginations that form into the early endosome lumen, eventually leading to the formation of multivesicular endosomes, herein referred to as endosomal carrier vesicles/multivesicular bodies (ECVs/MVBs) (Gruenberg and Stenmark, 2004), which then detach—or mature—from early endosomes. Eventually, intralumenal vesicles are delivered to late endosomes and lysosomes, where degradation occurs, or to the extracellular medium as exosomes (Trajkovic et al., 2008). Alternatively, they can release their content into the cytoplasm by undergoing back-fusion with the endosome limiting membrane (van der Goot and Gruenberg, 2006).

Major membrane remodeling occurs during ECV/MVB biogenesis, but the process is poorly understood. The mechanism that controls the invagination process itself is not clear, and it may depend on PtdIns3P, ESCRT I, ESCRT II, and ESCRT III complexes and their associated proteins, which sort signaling receptors into intralumenal vesicles (Williams and Urbe, 2007). However, transport from early to late endosomes continues when the invagination process is prevented by PtdIns3-kinase inhibition (Futter et al., 2001; Petiot et al., 2003), Snx3 knockdown (Pons et al., 2008), or Hrs knockout in *Drosophila* (Lloyd et al., 2002). Under these conditions, early-to-late endosome transport apparently occurs via endosomes that are no longer multivesicular ("empty" endosomes), indicating that the biogenesis of such intermediates can be uncoupled from the invagination process.

Conversely, we previously found that annexin A2 (AnxA2) depletion with siRNAs inhibits transport beyond early endosomes without interfering with the membrane invagination process (Mayran et al., 2003), suggesting that AnxA2 is involved in endosome biogenesis. AnxA2 is a member of the annexin family of calcium- and phospholipid-binding proteins, and it is present on early endosomes (Emans et al., 1993). In contrast to other annexins, however, AnxA2 binding to early endosomes is calcium independent, but cholesterol dependent, and this unique binding property requires the AnxA2 hypervariable N terminus (Harder et al., 1997; Jost et al., 1997). In addition, AnxA2 interacts with actin (Gerke and Weber, 1984; Hayes et al., 2004b), and it may play a role in actin-based macropinocytic rocketing (Merrifield et al., 2001) as well as in actin filament dynamics via monomer sequestration and barbed-end capping activities (Hayes et al., 2006) or, alternatively, via actin nucleation (Hayes et al., 2008). Evidence is in fact accumulating that, in addition to the well-established role of microtubules, actin is involved in membrane trafficking, including in the endocytic pathway (Kaksonen et al., 2006; Soldati and Schliwa, 2006). Actin was shown to play a role in transport toward lysosomes (Durrbach et al., 1996; Taunton et al., 2000) together with myosin 1B, which is involved in the sorting of the protein cargo Pmel17 into multivesicular endosomes (Salas-Cortes et al., 2005).

The precise role of actin in endosome dynamics is not clear, and several not mutually exclusive scenarios can be evoked. They include regulated endosome anchoring onto the actin network at the cell periphery, remodeling of the actin network by endocytic vesicles along their trajectory, endosome motility

along existing actin filaments, and possibly rocketing via de novo F-actin formation. Alternatively, actin may play an active role in membrane remodeling during endosome biogenesis. Little is also known about the mechanisms that control physical interactions between actin and endosomal membranes. Here, we have studied the role of actin in early-to-late endosome transport. We find that patches of F-actin are nucleated by early endosomes and are required for transport beyond early endosomes. Our data show that AnxA2 regulates actin nucleation in a process that depends on the actin nucleation factor Spire1 and the branching factor Arp2/3. We conclude that AnxA2 and Spire1 nucleate and stabilize F-actin, which, in turn, facilitates the necessary membrane remodeling that accompanies endosome biogenesis.

## RESULTS

### Actin Polymerization Is Required for Early-to-Late Endosome Transport In Vivo

It is now widely accepted that actin filaments are involved in internalization from the plasma membrane, including in the formation of at least some populations of clathrin-coated vesicles (Kaksonen et al., 2006; Mayor and Pagano, 2007; Soldati and Schliwa, 2006). However, much less is known about the possible role of F-actin at the next step of the pathway, during transport from early to late endosomes. To monitor endocytosis, we used rhodamin-dextran as a fluid-phase tracer. After a 10 min incubation at 37°C, the tracer reached early endosomes containing the Rab5 effector EEA1 (see Figures S1A and S1B available online). When actin polymerization was prevented by preincubation with latrunculin B (LatB) for 30 min, dextran internalization into EEA1-positive endosomes continued, albeit less efficiently (Figures S1A and S1B) as expected (Mayor and Pagano, 2007; Soldati and Schliwa, 2006).

When control cells were further incubated for 40 min at 37°C in fresh medium after the dextran pulse, the tracer no longer colocalized with EEA1 (Figure 1A, quantification in Figure 1B) and reached late endosomes containing Lamp1 (not shown) (Petiot et al., 2003). In marked contrast, however, dextran remained in early endosomes containing EEA1 in LatB-treated cells (Figure 1A, quantification in Figure 1B), failing to reach late endosomes. The actin-depolymerization agent cytochalasin D also inhibited early-to-late endosome transport, albeit to a lesser extent, whereas the F-actin-stabilizing agent jasplakinolide had no effect (Figures S1C and S1D). Individual endosomes could easily be detected after each treatment, including LatB (Figure S2B): the number of endosomes per unit surface area was similar in all cases (Figure S2C). Similarly, after EGF stimulation of LatB-treated cells, the EGF receptor remained in early endosomes and did not reach late endosomes, in contrast to controls (Figure S3), and, consistently, its degradation was delayed (Figure 1C). This delay did not result from LatB toxicity, since the effects were fully reversible (Figure S2A) and cell viability was not affected after drug washout (not shown).

### Ultrastructure of Endosomes after Actin Depolymerization

To gain further insights into the precise role of actin, we analyzed the ultrastructure of endosomes after HRP endocytosis for 10 min at 37°C followed by a 40 min chase. In control cells, HRP distributed mainly within isolated vesicles with the characteristic appearance of ECV/MVBs (Figure 1D, quantification in Figure 1E), as previously observed (Gruenberg et al., 1989; Mayran et al., 2003; Pons et al., 2008). In LatB-treated cells, far fewer characteristic ECVs were observed, and HRP was mostly present within structures with the typical tubulovesicular and cisternal appearance of early endosomes (Figure 1D, quantification in Figure 1E). However, intralumenal vesicles could still be observed in the vesicular regions of LatB-treated early endosomes, despite the inhibition of ECV/MVB biogenesis. Actin thus seems to control ECV/MVB formation from early endosomes, but not intralumenal membrane invagination.

### The Formation of an Endosomal Transport Intermediate Requires Actin Polymerization

Since actin polymerization seemed to be required for transport beyond early endosomes, we investigated whether polymerized actin plays a direct role in ECV/MVB formation—or maturation. We used an in vitro assay that reconstitutes ECV/MVB formation from donor early endosomes (Aniento et al., 1993; Mayran et al., 2003; Petiot et al., 2003). Cells were incubated with the bulk phase marker horseradish peroxidase (HRP) for 5 min at 37°C to label early endosomes. These were subsequently purified by subcellular fractionation and were incubated with cytosol and ATP at 37°C. ECV/MVBs that may have formed in vitro were then separated from donor membranes by floatation in step sucrose gradients. Strikingly, ECV/MVB formation was reduced when actin polymerization was prevented by LatB during the in vitro reaction (Figure 1F). Actin polymerization thus seems to be required for early-to-late endosome transport, and it may play a direct role in the formation of transport intermediates from early endosomes.

### Dynamic Actin Patches Can Be Observed on Early Endosomes

Next, we investigated the relationships that may exist between actin and early endosome dynamics in vivo. HeLa cells were fixed 10 min after incubation with rhodamin-dextran to label early endosomes, and F-actin was labeled with phalloidin. As previously reported (Nielsen et al., 1999), endosomes containing dextran were frequently observed along actin cables (Figure S4A, open arrowheads). To determine the role of these interactions, we followed the dynamics of early endosomes and F-actin after cotransfection with $Rab5^{GFP}$ and $actin^{RFP}$ by time-lapse microscopy. Consistent with previous studies (Nielsen et al., 1999), some, but not all, early endosomes labeled with $Rab5^{GFP}$ exhibited long-range movement at the rate (see Figures S4B and S4C, $\approx 0.2\ \mu m/s \pm 0.05$) expected for microtubule-based motility (Soldati and Schliwa, 2006). We also found that endosomes capable of moving over long distances were not associated with actin cables (motility was not changed by drugs that affect actin, Figure S4E) and, conversely, that endosomes, which localized to actin cables, remained essentially stationary (Figure S4D, average rate of $\approx 0.015\ \mu m/s \pm 0.009$). These observations suggest that early endosomes, which have the capacity to move along microtubules (Nielsen et al., 1999), can be immobilized by prolonged interactions with actin cables.

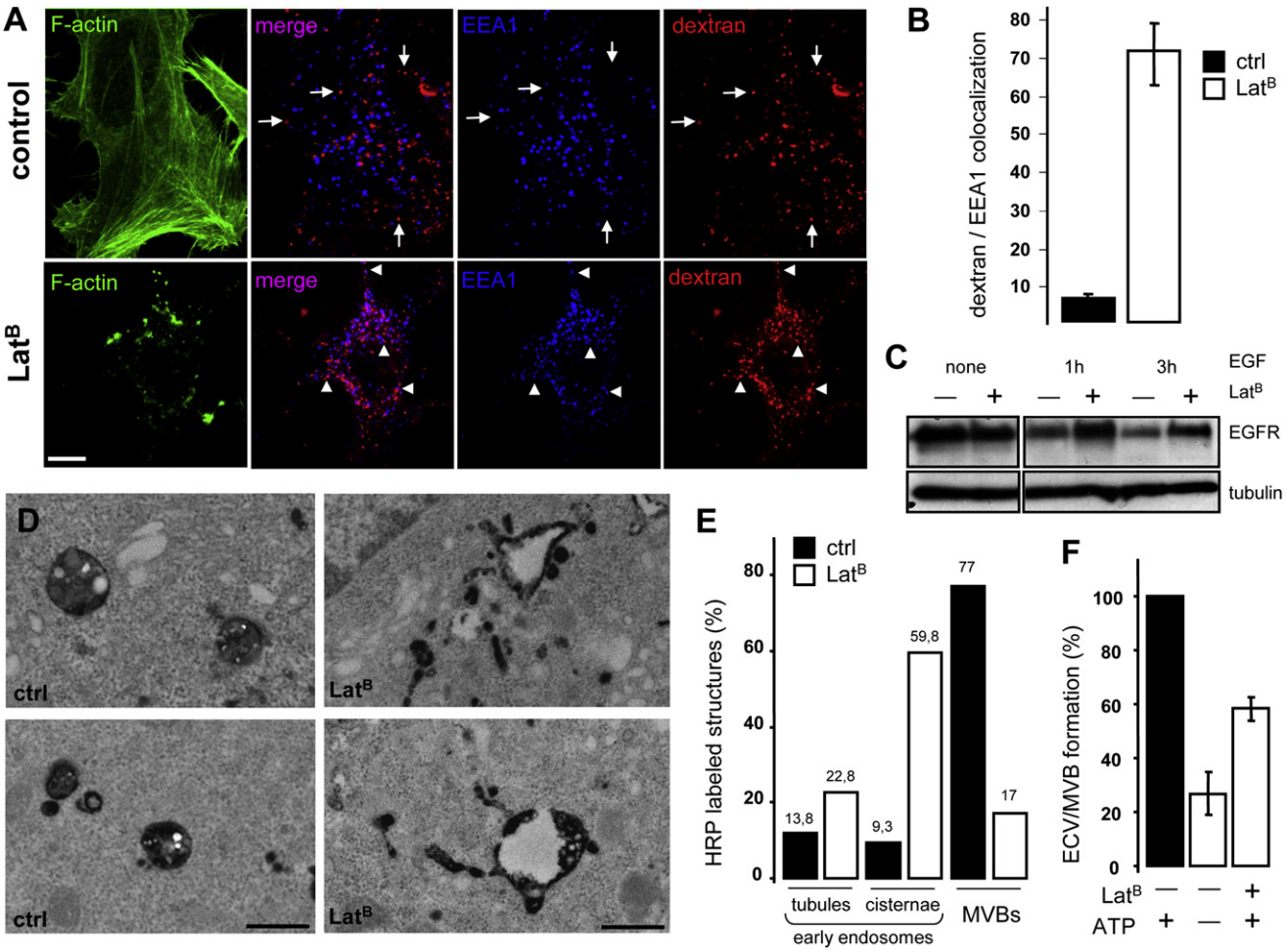


**Figure 1. Requirement of Actin Polymerization for Endosomal Transport**

(A) HeLa cells were incubated without or with 1 μM LatB for 30 min. Then, rhodamin-dextran was internalized for 10 min at 37°C and chased in the presence of LatB for 40 min. Cells were fixed and labeled with phalloidin (green channel) and antibodies against EEA1, followed by secondary antibodies (blue channel). Arrows point to dextran-labeled endosomes that do not contain EEA1 in controls, and arrowheads point to dextran-labeled endosomes that still contain EEA1 in cells treated with LatB. The scale bar represents 10 μm.

(B) The number of structures containing both dextran and EEA1 after chase in (A) is expressed as a percentage of the total number of dextran vesicles with or without LatB (n = 5, five cells per condition and ten structures per cell, ± SD).

(C) BHK cells treated or not with LatB for 30 min and then for 1 hr in serum-free medium were stimulated or not with EGF for 1 hr or 3 hr with or without LatB, lysed, and analyzed by SDS-PAGE and western blot.

(D) BHK cells were treated (LatB) or not (controls, ctrl) with LatB as in (A). HRP was internalized for 5 min at 37°C and then chased for 30 min. Cells were processed for electron microscopy. The scale bar represents 500 μm.

(E) In (D), ten cell profiles were chosen randomly, and the number of HRP-labeled tubules, cisternae, or multivesicular bodies (MVBs) were counted and expressed as a percentage of total HRP-labeled structures in each category.

(F) ECV/MVB formation was measured in vitro with or without ATP and LatB. The mean of four experiments ± SD is shown and is expressed as a percentage of control (+ATP).

In addition to the capture of early endosomes by actin cables, we also observed small, cloud-like patches of polymerized actin that protruded from or embedded early endosomes containing endocytosed dextran (Figure S4A, solid arrowheads). Such small actin$^{RFP}$ patches were frequently observed on endosomes labeled with Rab5$^{GFP}$ in vivo. Typically, these actin patches consisted of short filaments and were clearly distinct from large actin bundles (Figure 2A; also compare the upper and lower panels in Figure S4A). The presence of actin patches was not due to its overexpression. The number of early endosomes decorated with actin patches was essentially identical when endogenous actin was visualized with phalloidin (see below), and no significant difference in the patch size was observed with actin$^{RFP}$ or with phalloidin (not shown). Evidence for a specific interaction came from the observations that actin patches and endosomes remained associated in time during movement (Figure 2A). Patches were often observed at sites at which endosome fission occurred (Figure 2B; Movie S1), or in endosome-endosome

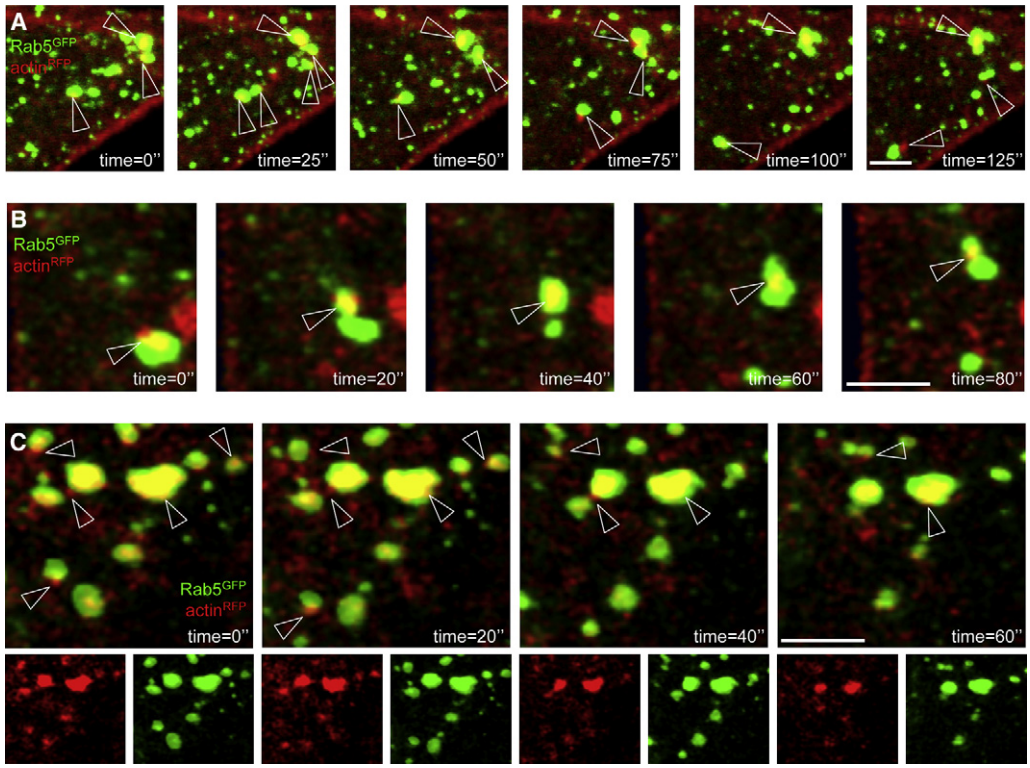


**Figure 2. Actin Structures Associated with Early Endosomes**

(A–C) HeLa cells were cotransfected with Rab5$^{GFP}$ and actin$^{RFP}$. Frames were captured every (B and C) 20 s or (A) 25 s by time-lapse confocal microscopy. Arrowheads point to actin patches associated with endosomes in time. The scale bars represent 5 μm.

interactions, including perhaps fusion (Figure 2C; Movie S2), raising the possibility that they play a role in endosomal membrane dynamics.

## Electron Microscopy Analysis of Endosomal Actin Patches

When analyzed by electron microscopy in MDCK cells (see Supplemental Data), clearly defined filamentous material was observed in association with the cytoplasmic surface of early endosomes, which had been labeled with HRP endocytosed for 10 min at 37°C (Figure 3A, open arrows). Early endosomes with this filamentous material also frequently showed a coat resembling the clathrin-Hrs coat that mediates ubiquitinated receptor sorting into early endosomes (Figure 3A, arrowheads) (Williams and Urbe, 2007).

After labeling early endosomes with BSA-gold internalized for 15 min at 37°C, cells were processed by using a freeze substitution protocol and embedded in Lowicryl resins HM20. Then, filamentous material was clearly apparent even at very low magnification (Figure 3C, open arrow) and was more obvious than in Epon sections (compare with Figure 3A). The electron-dense material associated with the periphery of the endosomal vacuole formed a brush-like electron-dense coat of fine filaments radiating out ~50–100 nm from the endosome surface. This filamentous material was found associated to ≈52% ± 5% of HRP-labeled endosomes—a value in good agreement with our quantification of endosome-associated actin patches by light microscopy (not shown)—but not with late endocytic compartments (Figure 3C) or other cellular membranes (not shown). Strikingly, filaments were efficiently labeled with anti-actin antibodies (Figure 3B, small arrowheads); essentially all filamentous structures associated with endosomes were labeled with anti-actin antibodies. Presumably, these short actin filaments associated with early endosomal membranes correspond to the dynamic actin patches observed by light microscopy.

## Purified Endosomes Support Actin Polymerization In Vitro

Next, we used an in vitro approach to investigate whether endosomes could drive actin nucleation and polymerization in vitro. Early endosomes purified from BHK cells expressing Rab5$^{GFP}$ were incubated with complete BHK cytosol at 37°C. After fixation, F-actin was labeled with phalloidin, and both endosomes and actin were analyzed by fluorescence microscopy. Immediately after mixing, endosomes labeled with Rab5$^{GFP}$ were readily observed, but they were essentially devoid of F-actin (Figure 4A, t = 0 min). By contrast, after a 2 min incubation at 37°C, actin filaments were seen growing from early endosomes (Figure 4A, t = 2 min), indicating that purified endosomes can trigger actin polymerization. Already after 2 min, ≥80% Rab5-labeled endosomes had triggered actin nucleation/polymerization, and this value did not change much after longer incubation (Figure 4F). However, these short filaments rapidly grew in length and sometimes became interconnected or branched, eventually forming a filamentous network (Figure 4A, t = 15 min and t = 30 min) that presumably reflected unbalanced actin dynamics in vitro.

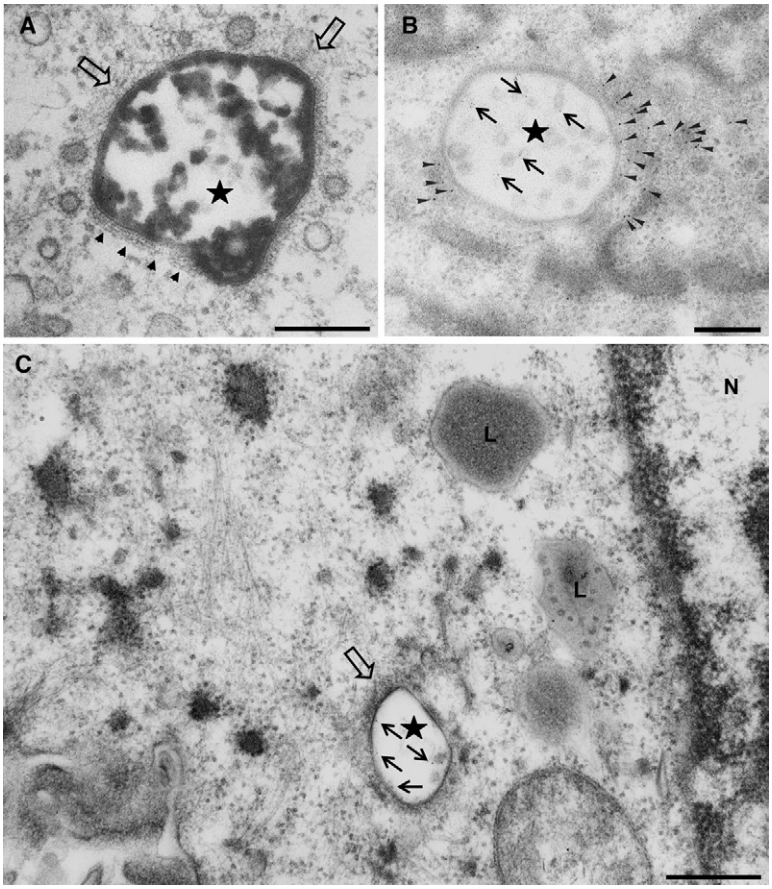


**Figure 3. Electron Microscopic Analysis of Endosomal Actin**

(A) MDCK cells grown on filters were incubated with HRP in apical and basolateral media for 10 min at 37°C and were processed for electron microscopy. The panel shows a multivesicular early endosome (star) with a filamentous coat (open arrows) and the characteristic clathrin bilayered coat (arrowheads).

(B) Cells were incubated as in (A), but with 5 nm BSA-gold (arrows), fixed, cryoprotected, freeze substituted, and embedded in Lowicryl K4M at low temperature. Sections were labeled with antibodies to actin and 10 nm proteinA gold (arrowheads).

(C) Cells were processed as in (B), except that they were embedded in Lowicryl HM20 at low temperature. An early (solid star), but not a late (L), endosome containing BSA-gold (arrows) shows the characteristic filamentous coat (open arrow). N, nucleus.

The scale bars represent 200 nm.

Without endosomes, some de novo, LatB-sensitive actin polymerization could be observed (not shown), but the process was greatly facilitated by the presence of early endosomes (Figure 4A). Indeed, early endosomes significantly increased phalloidin fluorescence intensity in randomly selected microscope fields (Figure 4B) when compared to cytosol alone (Figure 4C), as well as total F-actin polymerization (Figure 4E) and the length of filaments (Figure 4G). This was not simply due to the presence of membranes in the reaction mixture. Phalloidin fluorescence (Figure 4D), total F-actin polymerization (Figure 4E), and filament length (Figure 4G) were all significantly reduced when the early endosome fraction was replaced with a heavy membrane fraction from the same gradient, which contains primarily early biosynthetic membranes (Aniento et al., 1996). Finally, the early endosome-dependent nucleation (Figure 4F) and polymerization (Figure 4G) of actin filaments required ATP and was inhibited by LatB, as expected, and by EDTA, consistent with the notion that calcium-binding proteins are required (Pollard, 2007). Altogether these observations indicate that early endosomes may have the intrinsic and specific capacity to trigger the nucleation or polymerization of actin filaments.

## AnxA2 Distribution and Actin Patches

Our observations indicate that F-actin is necessary for early-to-late endosome transport, and that early endosomes stimulate F-actin polymerization. It is thus tempting to speculate that transport in the pathway is controlled by actin nucleation and polymerization on the early endosome surface. When searching for proteins that may play a role in these interactions, AnxA2 appeared as an interesting candidate, since this protein interacts with actin (Hayes et al., 2004b) and is found on early endosomes (Emans et al., 1993; Mayran et al., 2003; Morel and Gruenberg, 2007); 80% of the AnxA2-positive structures also contained Rab5 and 77% contained EEA1. Moreover, AnxA2 is involved in endocytic membrane transport (Mayran et al., 2003; Morel and Gruenberg, 2007; Zobiack et al., 2003). Consistently, AnxA2 was found closely associated with small F-actin patches that also contained the ERM protein moesin (Figure S5A), in agreement with our previous observations that AnxA2, actin, and moesin are part of the same protein complex (Harder et al., 1997). Moreover, we found that after endosome purification by floatation in gradients, some actin could be coimmunoprecipitated with endosome-associated, GFP-tagged AnxA2 (Figure 5A), further supporting the notion that both proteins are associated on early endosome membranes.

The early endosome is highly pleiomorphic with tubular, cisternal, and vesicular elements that are frequently connected to each other (Gruenberg, 2001), and it is difficult to evaluate this organization by light microscopy. In order to provide higher spatial resolution, cells were transfected with the mutant $Q_{79}L$ of Rab5, which causes the formation of enlarged early endosomes (Pons et al., 2008; Raiborg et al., 2002; Trajkovic et al., 2008). F-actin could be observed on these enlarged endosomes (Figure 5B; Figure S5D). The size of the actin patches was very similar to that observed after expression of Rab5 (not shown), and the percentage of endosomes decorated with actin patches was essentially identical upon expression of $Rab5^{GFP}$ or $Rab5Q_{79}L^{GFP}$ (not shown). Actin, but not $Rab5Q_{79}L^{GFP}$ itself, was distributed in a nonhomogeneous manner, within 1–2 patches per endosome (Figure S5D, arrowheads). AnxA2 was also present on the surface of these enlarged early endosomes (Figure 5B) and, much like actin, seemed to be nonhomogeneously distributed on the vesicle membrane (Figure 5B), in agreement with our previous analysis by electron microscopy

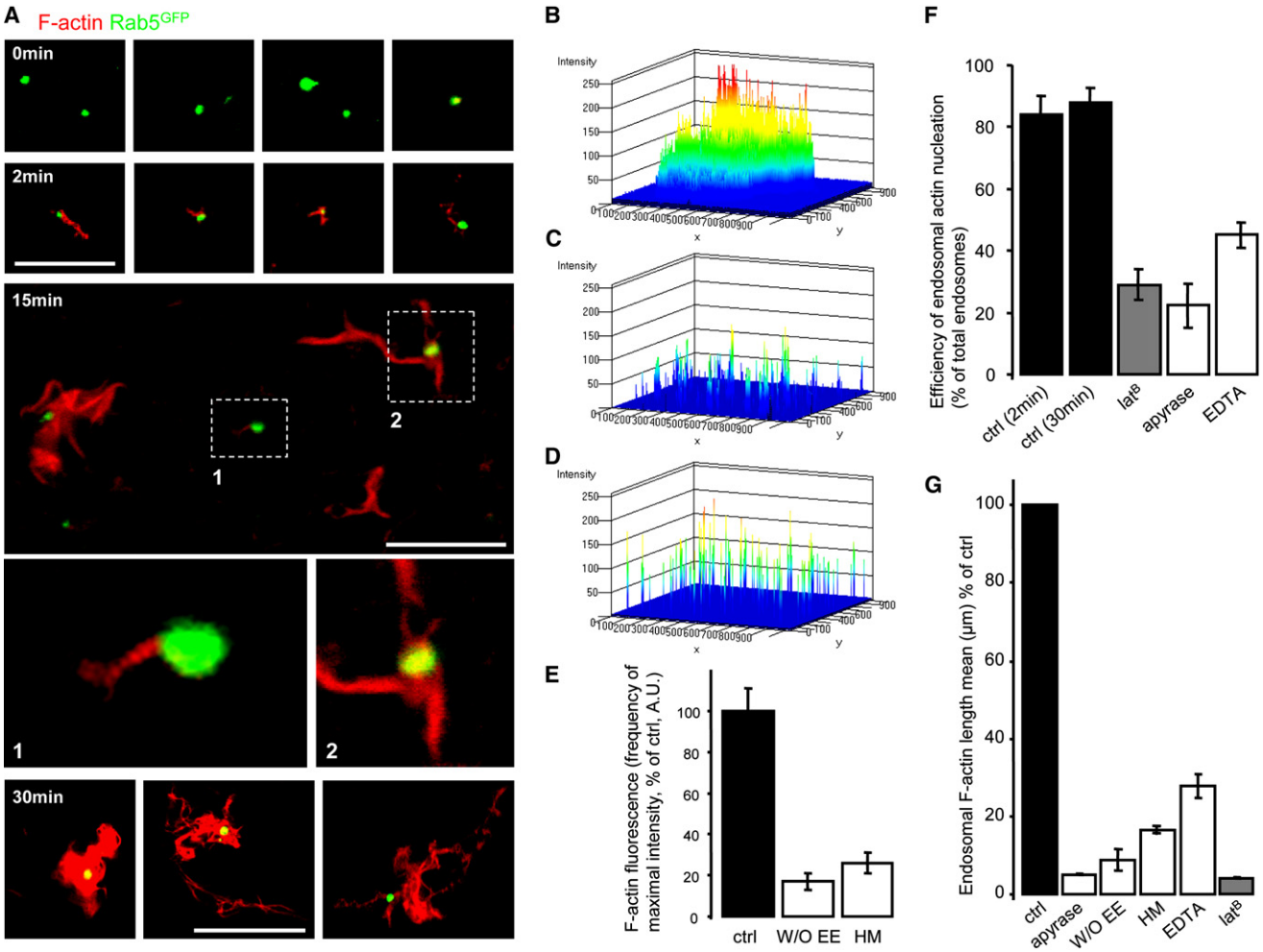


**Figure 4. Induction of In Vitro Actin Polymerization by Isolated Early Endosomes**

(A) Early endosomes purified from cells expressing rab5$^{GFP}$ were mixed with BHK cytosol and ATP. The mixture was incubated as indicated, fixed, labeled with phalloidin, and analyzed by fluorescence microscopy. Scale bars represent 10 μm for the 0, 2, and 30 min panels and 5 μm for the 15 min panel.

(B) The panel shows the actin fluorescence intensity of each pixel over a 1024 × 1024 area in (A) after 30 min of incubation and is color coded from blue to red as intensity increases.

(C and D) The experiments were performed as described in (A) and (B), except that endosomes were (C) omitted or (D) replaced with a heavy membrane fraction from the same gradient (Aniento et al., 1993).

(E) The frequencies of maximal actin fluorescence intensity were quantified in (B)–(D) (n = 6, ±SD).

(F) Rab5$^{GFP}$ endosomes with associated (A) actin filaments were scored after a 2 min (ctrl 2 min) or 30 min incubation without (ctrl 30 min) or with LatB, EDTA, or apyrase (to deplete ATP). Values are expressed as a percentage of the total number of endosomes labeled with Rab5$^{GFP}$ (n = 8, ±SD).

(G) The length of actin filaments associated with single Rab5$^{GFP}$ endosomes was measured without (ctrl) or with LatB, EDTA, and apyrase. Alternatively, endosomes were omitted (w/o EE) or replaced with heavy membranes (HM). The mean values are expressed as percentages of the total number of ctrl endosomes (n = 10, ±SD).

(Harder et al., 1997). AnxA2 was observed at sites from which actin patches seem to protrude from the endosome (Figure 5B, arrowheads). AnxA2 and actin codistributed on ≈50% of the total number of endosomes containing AnxA2, which is likely to be an underestimate, because of the complex three-dimensional organization of endosomes.

## AnxA2 Is Required for Actin Patch Nucleation In Vivo

We had previously reported that AnxA2 knockdown with synthetic (Mayran et al., 2003) or Dicer-generated (Morel and Gruenberg, 2007) siRNAs inhibited early-to-late endosome transport (see Figures S5B and S5C), without affecting earlier steps of the pathway. Typically, our electron microscopy study had shown that AnxA2 knockdown prevents ECV/MVB detachment from early endosomes and thus inhibits transport beyond early endosomes, without interfering with intralumenal vesicle formation (Mayran et al., 2003). Strikingly, these effects of AnxA2 knockdown could be fully recapitulated by actin depolymerization with LatB (see above; Figures 1D and 1E); free ECV/MVBs failed to undergo fission—or mature—from early endosomes. Consistent with the notion that fission was inhibited, the size of early endosomes was increased upon

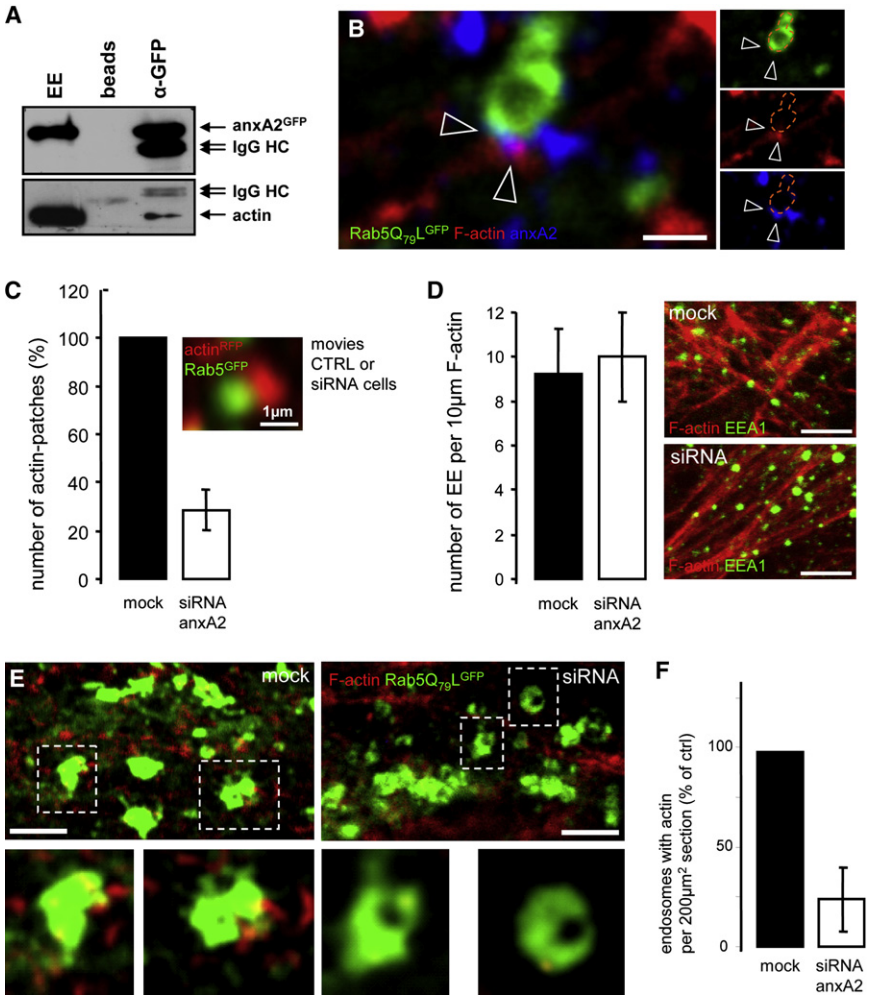


**Figure 5. AnxA2 and Endosomal Actin Patches In Vivo**

(A) AnxA2$^{GFP}$ was immunoprecipitated with (α-GFP) or without (beads) anti-GFP antibodies from early endosomes (EE as starting materials) prepared from cells transfected with AnxA2$^{GFP}$. Samples were analyzed by SDS-PAGE and western blot with antibodies against GFP or actin (the IgG heavy chain is indicated).

(B) HeLa cells transfected with Rab5Q$_{79}$L$^{GFP}$ were processed for confocal immunofluorescence after labeling with phalloidin and anti-AnxA2 antibody. Arrowheads point to F-actin and AnxA2, on the endosome surface (dotted lines). The scale bar represents 1 μm.

(C) HeLa cells were cotransfected with WT Rab5$^{GFP}$ and actin$^{RFP}$ (Figure 2) and AnxA2 was (siRNA AnxA2) or was not (mock) depleted. The number of actin patches on the surface or motile Rab5$^{GFP}$ endosomes filmed in vivo was measured per 1000 μm$^2$ area of cell cytoplasm in the confocal section. Data are expressed as a percentage of the mock-treated control ± SD. The scale bar represents 1 μm.

(D) The number of EEA1-positive endosomes attached to actin cables labeled with phalloidin was measured per 10 μm cable length after AnxA2 depletion as in (C). The mean values are shown ± SD. Scale bar represents 4 μm.

(E and F) (E) AnxA2 was (siRNA AnxA2) or was not (mock) depleted in HeLa cells, and then cells were transfected with Rab5Q$_{79}$L$^{GFP}$. Single endosomes present in the boxed areas are cropped and shown below. The scale bar represents 2 μm. (F) The number of actin patches on endosomes was measured per 200 μm$^2$ area of cell cytoplasm in the confocal section and is expressed as a percentage of the mock-treated control ± SD.

AnxA2 knockdown (Figure S6E). Altogether, these observations strongly suggest that AnxA2 and actin are required at the same step, during ECV/MVB formation from early endosomes.

Under our conditions, AnxA2 depletion did not cause major changes in the organization of the actin cytoskeleton. Total actin (Figure S6A) and the general organization of actin fibers (Figure S6C) were not altered. Similarly, cell shape was not changed, as measured from the cell perimeter (Figure S6B), in contrast to a previous study with Müller glial cells (Hayes et al., 2006); this discrepancy may reflect the more dynamic physiology of glial cells (Hayes et al., 2006) when compared to our HeLa cells. We next quantified the actin patches on motile early endosomes to ensure that only specific association was being monitored. Strikingly, the number of patches was significantly decreased upon AnxA2 knockdown (Figure 5C; Movies S3 and S4 show mock- and siRNA-treated cells, respectively). By contrast, the number of immobile endosomes captured by actin cables (see Figure S4A) was not affected (Figure 5D). Neither was the motility of early endosomes labeled with Rab5$^{GFP}$ (Figure S6D). Finally, the formation of actin patches on enlarged endosomes induced by Rab5Q$_{79}$L$^{GFP}$ expression was reduced >4-fold after AnxA2 knockdown (Figure 5E, quantification in Figure 5F). Altogether, these observations demonstrate that AnxA2 is required for the formation of actin patches on dynamic early endosomes.

## Annexin A2 Is Essential for Actin Polymerization on Endosomes In Vitro

Our experiments unambiguously demonstrate that AnxA2 plays a role in endosome transport and F-actin nucleation/polymerization in vivo. However, siRNAs do not allow acute protein depletion, and it may be difficult to discriminate between direct and indirect effects of the depletion. We therefore made use of the property of annexin family members to be efficiently precipitated by high $CaCl_2$ concentrations (Rescher and Gerke, 2004), to deplete AnxA2 biochemically. After $CaCl_2$-mediated precipitation, cytosols were prepared that essentially lacked AnxA2, as well as other annexins, including AnxA1 and AnxA6 (Figure 6A). By contrast, actin and Rab5 were not affected (Figure 6A). Neither was p11/S100A10 (Figure 6A), which interacts with AnxA2 at the plasma membrane (Rescher and Gerke, 2004), but not on endosomes (Morel and Gruenberg, 2007).

In our in vitro assay (see Figure 4), the capacity of annexin-depleted cytosols to support F-actin nucleation and polymerization was reduced ≈4- to 5-fold, when compared to control

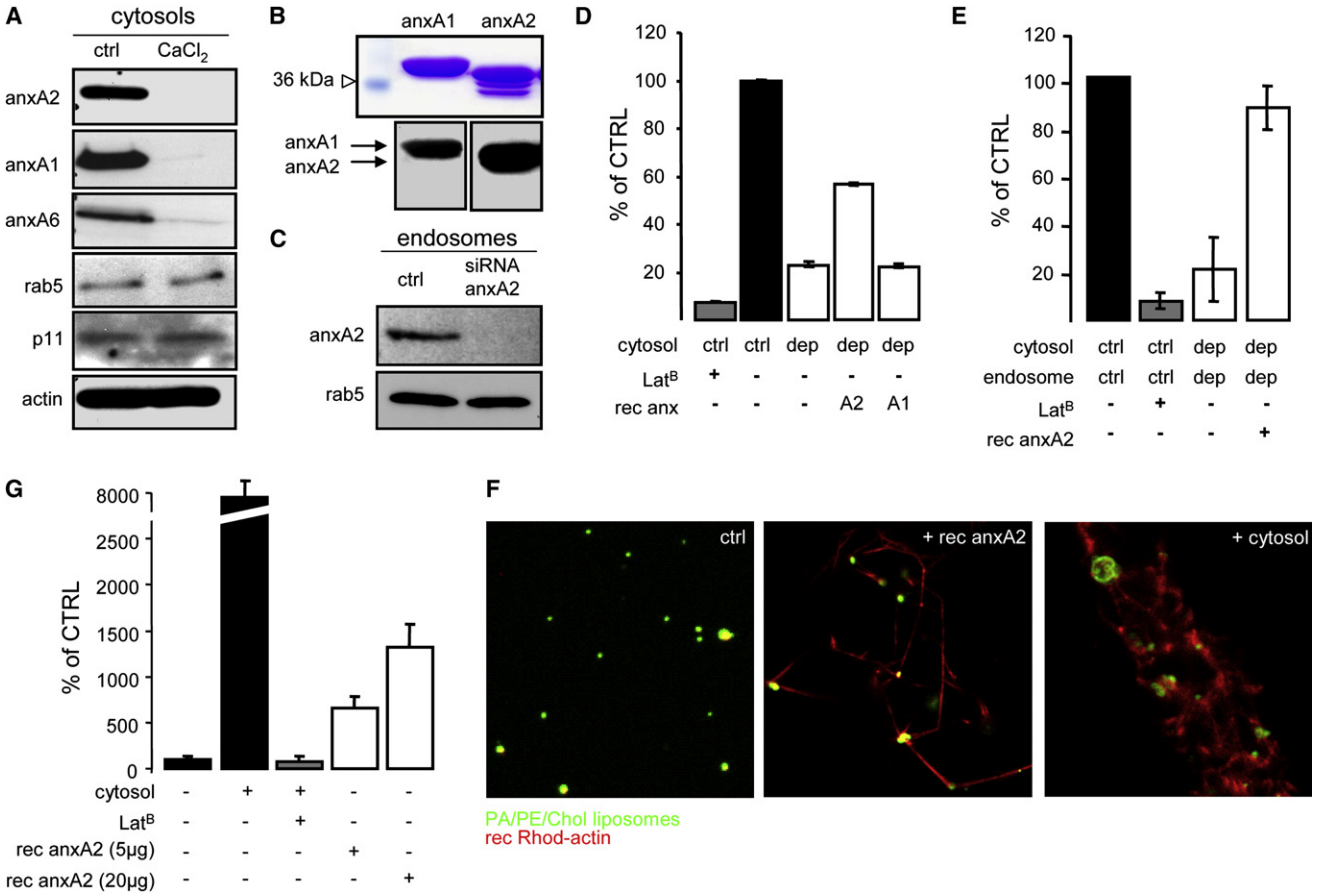


**Figure 6. AnxA2-Dependent Actin Polymerization on Endosomes and Liposomes**

(A) BHK cytosol isolated was treated or not with 1 mM $CaCl_2$ centrifuged at high speed, and the supernatants were analyzed by SDS-PAGE and western blot.

(B) Purified recombinant annexin A2 (AnxA2) and annexin A1 (AnxA1) were analyzed by SDS-PAGE (upper panel, Coomassie staining; lower panels, western blots).

(C) Endosomes from control (ctrl) or AnxA2-depleted (siRNA AnxA2) cells were analyzed by western blot.

(D) The in vitro assay was as described in Figure 4, in the presence of control cytosol (ctrl) or annexin-depleted cytosol (dep) prepared as described in (A). The assay was recomplemented with purified recombinant AnxA1 or AnxA2, or with LatB. Quantification as described in Figure 4G is expressed as a percentage of the control (n = 20, ± SD).

(E) The assay was as described in (D), except that endosomes were prepared from control (ctrl) or AnxA2-depleted (dep) cells, as in (C). Before the assay, endosomes were preincubated with AnxA2 for 30 min on ice, to allow for membrane reassociation.

(F) Liposomes stained with FM2-10 were mixed with 0.05 µg recombinant rhodamin-actin and 0.5 µg unlabeled actin. The mixture was not (ctrl, control) or was supplemented with BHK cytosol (+cytosol; 5 mg/ml final concentration) or 5 µg recombinant anxA2 (+rec anxA2), preincubated for 30 min on ice, and then incubated for 10 min at 37°C. The mixture was fixed immediately and analyzed by fluorescence microscopy.

(G) The assay was performed as described in (F) at the indicated AnxA2 concentrations. Quantification as described in Figure 4G is expressed as a percentage of the control (n = 3, ±SD).

cytosols (Figure 6D). When the depleted cytosols were recomplemented with purified recombinant AnxA2 (Figure 6B), F-actin nucleation and polymerization could be partially restored (Figure 6D) in a dose-dependent manner (Figure S6F). By contrast, purified, recombinant AnxA1 (Figure 6B), which is related to AnxA2 and shows a similar structural organization and distribution on early endosomes (Rescher and Gerke, 2004), did not restore F-actin nucleation and polymerization in our in vitro assay (Figure 6D). Moreover, endosome-free, cytosolic nucleation events were not affected when purified, recombinant AnxA2 was added to annexin-depleted cytosol, demonstrating that AnxA2 modulates actin nucleation solely from endosomal membranes (Figure S6G).

Since a significant fraction of AnxA2 is associated with endosomal membranes (Emans et al., 1993; Harder et al., 1997), we prepared endosomes from cells that had been depleted of AnxA2 with siRNAs and cotransfected with $Rab5^{GFP}$ (Figure 6C). The capacity of AnxA2-depleted endosomes to support F-actin nucleation and polymerization in our assay was reduced to ≈1/3 of the controls (Figure 6E; Figure S6H). The process could be nearly completely restored by the addition of purified, recombinant AnxA2 (Figure S6H); values were somewhat higher than in Figure 6D, presumably because the assay mixture had been preincubated for 30 min at 4°C to allow AnxA2 reassociation to depleted membranes. Finally, AnxA2 depletion from both cytosol and endosome abolished F-actin

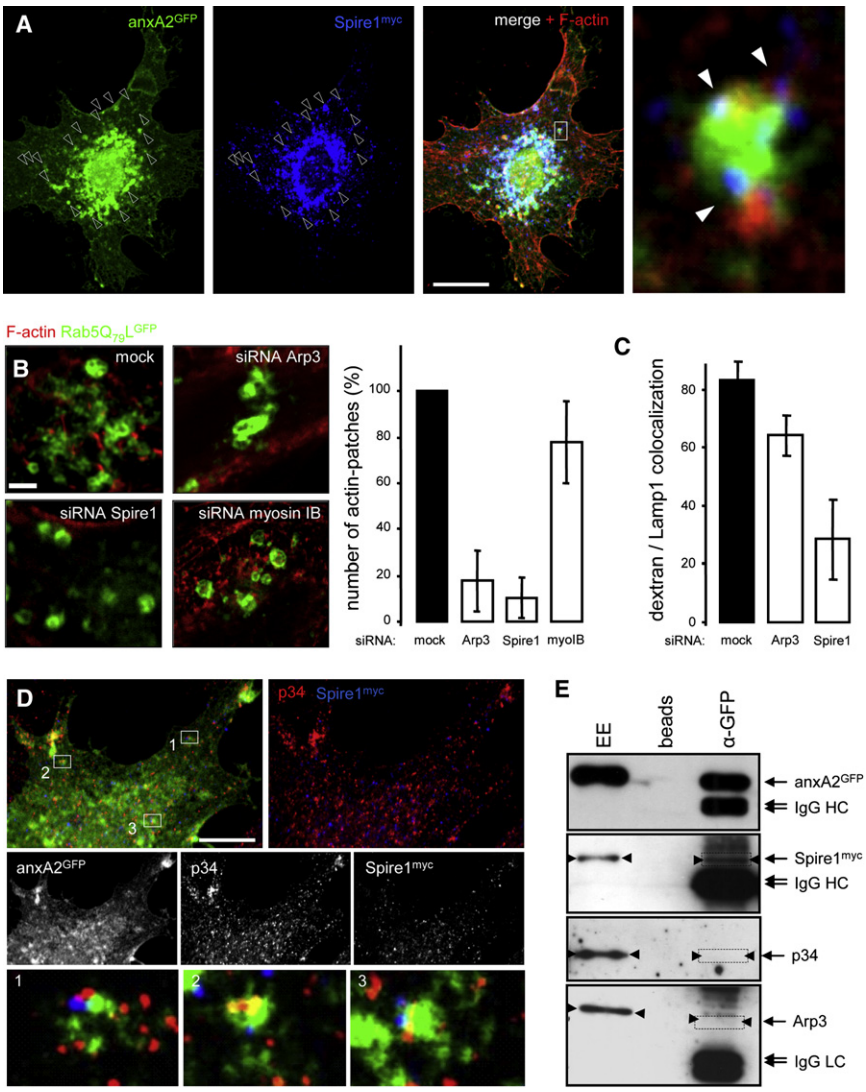


**Figure 7. Arp2/3 and Spire1 in Endosomal Actin Polymerization**

(A) HeLa cells transfected with anxA2$^{GFP}$ and Spire1$^{Myc}$ were labeled with anti-Myc antibody and rhodamin-phalloidin. Empty arrowheads show colocalization of anxA2$^{GFP}$ and Spire1$^{Myc}$, and white arrowheads (inset) show Spire1Myc/F-actin clustering on an anxA2$^{GFP}$ endosome. The scale bar represents 10 μm.

(B) Arp3, Spire1, or MyosinIB was depleted with siRNAs (see Figure S10) or not (mock), and then cells were transfected with Rab5Q$_{79}$L$^{GFP}$, fixed, and labeled with rhodamin-phalloidin. The scale bar represents 1 μm. The number of actin patches on endosomes was measured per 200 μm$^2$ area of cell cytoplasm in the confocal section and is expressed as a percentage of the mock-treated control (n = 3, ±SD).

(C) Arp3 or Spire1 were depleted from HeLa cells with siRNA or not (mock), and then rhodamin-dextran was internalized for 10 min at 37°C and chased for 40 min at 37°C. Cells were fixed, processed for immunofluorescence, and labeled with anti-Lamp1 antibodies. The number of structures containing both dextran and Lamp1 is expressed as a percentage of the total number of vesicles containing dextran in each condition. (n = 3, four cells per condition and six structures per cell, ±SD).

(D) HeLa cells transfected with anxA2$^{GFP}$ and Spire1$^{Myc}$ were labeled with anti-Myc antibody and anti-p34-Arc antibody. Insets show clustering and the close vicinity of p34-Arc and Spire1$^{Myc}$ on endosomes containing anxA2$^{GFP}$. The scale bar represents 20 μm.

(E) AnxA2$^{GFP}$ was immunoprecipitated with (α-GFP) or without (beads) anti-GFP antibodies from early endosomes (EE as starting materials) prepared from cells transfected with AnxA2$^{GFP}$ and Spire1$^{Myc}$. Samples were analyzed by SDS-PAGE and western blot with antibodies against GFP, Myc, p34-Arc, or Arp3 (IgG heavy and light chains are indicated).

nucleation and polymerization—to the same extent as did LatB—and the process could be restored by AnxA2 addition (Figure 6E). Strikingly, purified recombinant AnxA2 bound to liposomes (Mayran et al., 2003; Morel and Gruenberg, 2007), which may recapitulate the biochemical properties of AnxA2 on endosomes, was sufficient to trigger the polymerization of purified recombinant actin in a dose-dependent manner (Figure 6F, quantification in Figure 6G), demonstrating that membrane-associated AnxA2 has the intrinsic capacity to nucleate or stabilize actin filaments. However, filament formation was very inefficient when compared to complete cytosol (Figures 6F and 6G), and individual filaments appeared unbranched (Figure 6F), strongly suggesting that other factors are involved. Hence, we conclude that AnxA2 is necessary for the nucleation and the subsequent polymerization of actin onto early endosomal membranes, and that other factors are also likely to be involved.

## Annexin A2 and Actin Regulators

Actin partners or regulators that may play a role on endosomes include moesin, which colocalizes (Figure S5A) and interacts (Harder et al., 1997) with AnxA2, and myosin IB, which is present on early endosomes and is involved in endosomal traffic (Salas-Cortes et al., 2005). In contrast to AnxA2 knockdown (Figure 5E), myosin1B knockdown (see Figures S8D and S8E) did not significantly affect the number of actin patches present on endosomes enlarged by Rab5Q$_{79}$L$^{GFP}$ (Figure 7B), suggesting that this class I myosin acts at a more distal step in transport; we were not able to pursue the study of moesin because siRNAs were lethal.

We reasoned that Arp2/3 might play a role in filament branching (Pollard, 2007) during patch formation. Indeed, p34-Arc was found partially associated with AnxA2 on endosomes (Figure 7D), and Arp3 knockdown (Figures S8B and S8E) reduced the number of patches on enlarged endosomes (Figure 7B). Moreover, Arp3 depletion caused a small, but significant, reduction in the transport of a pulse of endocytosed dextran to late endocytic compartments containing Lamp1 (not shown; quantification in Figure 7C), suggesting that the Arp2/3 complex contributes to the formation of the endosomal actin patches. Interestingly, the actin-nucleating protein Spire1 (Quinlan et al., 2005) colocalized with vesicular actin (Figure S7A), AnxA2

(Figure 7A; Figure S8A), and, to some extent, with p34-Arc on endosomal structures (Figure 7D). Moreover, subcellular fractionation experiments showed that Spire1 copurifies with AnxA2 in early endosomes, whereas Arp2/3 was not significantly enriched in endosomes, consistent with its broader cellular distribution (Figures S7B and S7C). Finally, coimmunoprecipitation experiments showed that Spire1 interacts physically with endosomal AnxA2 (Figure 7E). Silencing of Spire1 (Figures S8C and S8E) prevented the formation of actin patches on enlarged early endosomes (Figure 7B) and inhibited dextran transport to late endosomes containing Lamp1 (Figure 7C); the more pronounced effects of Spire1 depletion as compared to Arp2/3 may reflect a stronger inhibition of actin patch formation, but they may also suggest that other mechanisms are at play (Figure 7B). We conclude that, together with AnxA2, Spire1 and Arp2/3 are involved in the dynamics of endosomal actin during ECV/MVB biogenesis.

## DISCUSSION

We find that cloud-like patches of F-actin are required for transport beyond early endosomes in a process that depends on AnxA2. Strikingly, actin depolymerization with LatB fully recapitulates the effects of AnxA2 depletion on endosome transport and morphology. Free ECV/MVBs then fail to detach or mature from early endosomes, without interfering with the formation of intralumenal vesicles, in marked contrast to Hrs or SNX3 depletion (Gruenberg and Stenmark, 2004; Pons et al., 2008). Our data also show that early endosomes trigger the nucleation and polymerization of actin filaments in vitro, and that this process depends on AnxA2, the nucleating factor Spire1 (Quinlan et al., 2005), and Arp2/3, which mediates filament branching (Pollard, 2007).

### Annexin, Actin, and Endosomes

AnxA2 shares with other members of its protein family the capacity to bind liposomes containing negatively charged phospholipids in a calcium-dependent manner. These interactions depend on the unique calcium-binding motif, which is repeated in the conserved C-terminal core domain (Rescher and Gerke, 2004). Consistently, AnxA2 interactions with the plasma membrane depend on calcium, but also on PtdIns(4,5)P2 (Hayes et al., 2004a; Rescher and Gerke, 2004). Similarly, AnxA2 interactions with the actin cytoskeleton are also calcium dependent (Rescher and Gerke, 2004), presumably accounting for our observations that actin polymerization on endosomes in vitro is sensitive to calcium chelation. By contrast, AnxA2 binding to early endosomes is calcium independent and cholesterol dependent, and this binding property requires the AnxA2 N-terminal domain (Harder et al., 1997; Jost et al., 1997; Mayran et al., 2003). Moreover, AnxA2 distributes on early endosomes in a nonrandom manner (Harder et al., 1997 and this study), consistent with observations that some annexins are endowed with the intrinsic ability to self-organize at the membrane surface into bidimensional ordered arrays (Oling et al., 2001), leading to the notion that AnxA2 forms platforms on early endosomal membranes (Mayran et al., 2003). It is attractive to propose that these platforms serve as the nucleation site for the polymerization of the short actin filaments associated with early endosomal membranes, which were observed by electron microscopy. Alternatively, AnxA2 platforms may also capture, anchor, and stabilize these short filaments.

### F-actin in Early Endosome Dynamics

Although future work will clearly be required to further elucidate the precise role of actin in early-to-late endosome transport, some speculations are already possible. Whereas the interaction of vesicles or compartments with cytoskeletal elements is generally associated with movement and thus transport, our observations indicate that actin-based motility does not play a major role in transport beyond early endosomes, but rather that actin drives the biogenesis of the transport intermediates. The movement of endosomes on actin cables and the rocketing of endosomes caused by de novo F-actin formation are unlikely to account for the actin- and AnxA2-dependent transport we have observed. Indeed, stationary and nonmotile endosomes interact with actin cables, and endosome rocketing on a comet tail of actin was not observed in our assay. Moreover, we find that the biogenesis of transport intermediates (ECV/MVBs) destined for late endosomes is inhibited by actin depolymerization or AnxA2 depletion. The movement of these intermediates during early-to-late endosome transport depends on intact microtubules, although how endosomal membranes acquire the capacity to interact with microtubules is far from clear (Soldati and Schliwa, 2006). Strikingly, however, F-actin depolymerization with LatB (this study) inhibits early-to-late endosome transport, at least to the same extent, if not more efficiently, than microtubule depolymerization with nocodazole (Gruenberg et al., 1989). And yet, actin-based endosome motility does not seem to play a direct role during transport toward late endosomes (Soldati and Schliwa, 2006), although actin may cooperate with microtubules in long distance transport. Lysosome motility and directionality are altered by a dominant-negative mutant of myosin 1B, and myosin 1B overexpression clusters multivesicular endosomes in the perinuclear region (Salas-Cortes et al., 2005). It is thus attractive to propose that, whereas microtubules facilitate endosome movement, F-actin may be necessary to engage the endosome maturation or transport process.

During transport beyond early endosomes, large ($\approx$0.5 $\mu$m diameter) and multivesicular endosomal intermediates (or ECV/MVBs) are formed from tubulocisternal early endosomes. This process involves concomitant deformation of the endosomal membrane in two opposite directions—toward the cytosol to generate the endosomal intermediate, and toward the endosomal lumen to form intralumenal vesicles (Gruenberg, 2001). Although major progress has been made in understanding protein sorting into ECV/MVBs (Gruenberg and Stenmark, 2004; Williams and Urbe, 2007), the mechanism responsible for membrane deformation during ECV/MVB biogenesis is poorly understood.

We wish to propose that short actin filaments nucleated or stabilized by AnxA2 on early endosomal membranes facilitate the membrane remodeling and subsequent severing process that accompanies the biogenesis of endosome intermediates (see model, Figure S9). We find that the formation of actin patches on early endosome depends on AnxA2 and Spire1, which interact with each other, as well as on Arp2/3. Spire1

may be recruited on early endosomal membranes by binding early endosomal PI3P via its FYVE-like domain (Kerkhoff et al., 2001), and may then be stabilized by interacting with AnxA2. In turn, endosomal Spire1 may stabilize the polymerization of actin filaments via G-actin monomer binding to its tandem WASP homology 2 domain (Kerkhoff et al., 2001; Rebowski et al., 2008). Clearly, AnxA2 may also facilitate the nucleation and polymerization reaction directly, in agreement with its known capacity to interact with actin. Next, Arp2/3 may mediate filament branching, presumably leading to the patches or plumes of actin observed by light and electron microscopy. Other proteins are likely to be involved in stabilizing actin patches on endosomes, including moesin (Harder et al., 1997 and this study). Finally, severing of the nascent ECV/MVB from recycling tubules and cisternae during the detachment or maturation process may be driven by actin assembly at the membrane and filament crosslinking or interactions with other actin-binding proteins, perhaps in a process akin to clathrin-coated vesicle formation in yeast (Kaksonen et al., 2006). Actin filaments may contribute to physically deform the ECV/MVB membrane by pulling onto AnxA2-rich domains and also by orchestrating the involvement of other necessary components in time and space, including interactions with microtubules. In conclusion, AnxA2 organized in specialized platforms contributes to nucleate, anchor, and stabilize actin filaments on early endosome membranes together with Spire1 and Arp2/3. Actin filaments in turn drive the formation of endosome transport intermediates, presumably by contributing to the membrane deformation and maturation process.

## EXPERIMENTAL PROCEDURES

### Cells, Antibodies, and Reagents

BHK21 and HeLa cell maintenance (Morel and Gruenberg, 2007) and transfection (Morel and Gruenberg, 2008) were described. The monoclonal antibody against Rab5 was a gift from R. Jahn (Göttingen, Germany); monoclonal antibodies against AnxA2 (HH7) and p11/S100A10 (H21) and rabbit polyclonal K419 antibody against AnxA2 were gifts from V. Gerke (Münster, Germany); and rabbit polyclonal antibody against moesin was a gift from P. Mangeat (Montpellier, France). The anti-actin antiserum (electron microscopy) was a gift of J. De Mey. Anti-Rab7 polyclonal antibody and anti-LBPA monoclonal antibody were described (Pons et al., 2008). Rabbit polyclonal antibodies were from the following sources: EEA1 from Alexis Biochemical; Lamp1 from Affinity Bioreagents; Arp3 from Cytoskeleton, Inc.; p34-Arc from Upstate. Monoclonal antibodies were from the following sources: GFP from Roche Diagnostics; EGF receptor from BD Biosciences; tubulin and cMyc (9E10) from Sigma; annexinA1, annexinA6, actin, and Myosin IB from Abcam Ltd.; Spire1 and Arp3 from Abnova. Peroxidase-conjugated secondary antibodies were from Bio-Rad, and Cy2-, Cy3-, and Cy5-conjugated fluorescent antibodies were purchased from Jackson Immunoresearch. Rhodamin-dextran (10,000 Da) and rhodamin-transferrin were from Molecular Probes. F-actin was labeled with Alexa Fluor coupled to phalloidin (Invitrogen). Latrunculin B ($Lat^B$) and cytochalasin D (CytD) were from Sigma, and jasplakinolide (JAS) was from Calbiochem.

### Plasmids, Recombinant Proteins, and RNAi

Plasmids were gifts from the following sources: human $AnxA2^{GFP}$ and porcine AnxA1, V. Gerke; $actin^{GFP}$ and $actin^{RFP}$, B. Ihmof (Geneva, Switzerland); $Rab5^{GFP}$ and $Rab5Q_{79}L^{GFP}$, M. Zerial (Dresden, Germany); tandem-FYVE, H. Stenmark (Oslo, Norway); Spire1-myc and $Spire1^{GFP}$, E. Kerkhoff (Regensburg, Germany). Recombinant AnxA2 and AnxA1 (Morel and Gruenberg, 2008) and AnxA2 downregulation were described (Morel and Gruenberg, 2007). The target sequences (all primers and sequences are listed in the 5′ to 3′ direction) for Arp3 downregulation are AAGTGGGTGATCAAGCTCAAA for siRNA1 and AAGCTCAAAGGAGGGTGATGA for siRNA2. For downregulation of Spire1 and myosin IB, we used the following QIAGEN predesigned siRNA: Hs-SPIRE1-10, CAGAGACGACATTCCATTGAA; Hs-SPIRE1-11, CAGGTGGAGGGTACGTTCATA; Hs-MYO1B-5, TAGGTGTATCAAACCGAATGA; and Hs-MYO1B-6, AACGAGCATTCAGTTTCCGAA.

### Endocytic Transport In Vivo

Cells preincubated or not with 1 μM $Lat^B$, CytD, or JAS in serum-free medium for 30 min were incubated with 3 mg/ml rhodamin-dextran for 10 min at 37°C in GMEM containing 10 mM HEPES, or were further chased for 40 min at 37°C, fixed, and processed for immunofluorescence (Morel and Gruenberg, 2007). Endocytic transport of the fluid-phase marker horseradish peroxidase (HRP) (Mayran et al., 2003) and EGF receptor (EGFR) was described (Pons et al., 2008).

### Actin Polymerization In Vitro

Purified $Rab5^{GFP}$ endosomes (final concentration ≈150 μg/ml) were mixed with the assay mixture: BHK cytosol (final concentration ≈5 mg/ml), 125 mM KCl, 20 mM HEPES (pH 7.0), 2.5 mM $MgOAc_2$, 1.6 mM DTT, and a cocktail of protease inhibitors (Gruenberg et al., 1989). Tubes were placed at 37°C without shaking, the reaction was stopped with 4% PFA on ice, polymerized actin was stained with Alexa Fluor 488 conjugated to phalloidin, and samples were analyzed by confocal microscopy. For quantification, the fluorescence intensity of each pixel was measured over a 1024 × 1024 pixels area, as were the length of actin fibers and the frequencies of maximal fluorescence intensity. Each parameter was always quantified manually via the Zeiss LSM software, and the statistical significance was determined with a Student's t test. Liposomes containing phosphatidic acid, phosphatidylethanolamine, and cholesterol (2:2:1) were described (Mayran et al., 2003; Morel and Gruenberg, 2007).

### Fluorescence Microscopy and Confocal Movies

In immunofluorescence experiments, sample preparation and analysis were always as described (Morel and Gruenberg, 2007, 2008). In movies, actin patches were quantified by counting the number of stable (from 2 to 5 min), small, and dynamic $actin^{RFP}$-labeled structures at the surface of $Rab5^{GFP}$ endosomes in 200 $\mu m^2$ focal planes. Actin patches were counted on the surface of enlarged endosomes induced by the expression of $Rab5Q_{79}L^{GFP}$ after F-actin staining with phalloidin. Actin patches were quantified in 200 $\mu m^2$ sections in the microscope. Each parameter (fiber length, distance, endosome diameter and number, cell perimeter, cell surface area, and actin fluorescence intensity) was quantified manually via the Zeiss LSM software.

### Electron Microscopy

The ultrastructure of endosomes treated with LatB was analyzed in Epon (Parton et al., 1992) and were quantified as described (Mayran et al., 2003). MDCK cells incubated in the apical and basolateral medium with 5 nm BSA-gold ($OD_{520}30$) or HRP (Sigma type II, 10 mg/ml) for 15 or 10 min at 37°C, respectively, were processed for Epon and then for freeze substitution (van Genderen et al., 1991) (see Supplemental Data). Lowicryl sections were labeled as described (Parton, 1994). After washing with PBS/BSA, the sections were treated briefly with 1% glutaraldehyde in PBS, washed with distilled water, and then stained with uranyl acetate in methanol followed by Reynold's lead citrate.

### Other Methods

BHK early and late endosomes and heavy membranes were prepared as described, as was BHK cytosol (±10 mg/ml final concentration) (Aniento et al., 1993). Total annexin depletion from cytosol with 1 mM $CaCl_2$ (Mayran et al., 2003) and ECV/MVB formation in vitro with or without 1 μM $Lat^B$ (Aniento et al., 1996; Mayran et al., 2003; Petiot et al., 2003) were described. Immunoprecipitation from total cell lysates or early endosomes was described (Morel and Gruenberg, 2007, 2008). Western blot was carried out by using the Super-Signal West Pico chemiluminescent substrate (Pierce Chemical Co.); exposure times were always within the linear range of detection.

## SUPPLEMENTAL DATA

Supplemental Data include Supplemental Experimental Procedures, Supplemental References, nine figures and four movies and can be found with this article online at http://www.cell.com/developmental-cell/supplemental/S1534-5807(09)00035-5.

## ACKNOWLEDGMENTS

We are grateful to Marie-Claire Velluz and Charles Ferguson for technical assistance and to Zeina Chamoun for AnxA2 siRNA duplexes and for comments on the manuscript. We are also grateful to Thierry Soldati, Gisou van der Goot, and Cameron Scott for critically reading the manuscript and to Eugen Kerkhoff for sharing reagents with us. Support was from the Swiss National Science Foundation; LipidX from the Swiss SystemsX.ch initiative, which was evaluated by the Swiss National Science Foundation; the Telethon Foundation; Phospholipid and Glycolipid Recognition, Interactions, and Structures by Magnetic Resonance (PRISM) from the European Union Sixth Framework Programme (to J.G.); the Human Frontier Science Foundation (R.G.P.); and the Fondation pour la Recherche Medicale (FRM) and the Roche Research Foundation (to E.M.).

Received: July 8, 2008
Revised: December 8, 2008
Accepted: January 20, 2009
Published: March 16, 2009

## REFERENCES

Aniento, F., Emans, N., Griffiths, G., and Gruenberg, J. (1993). Cytoplasmic dynein-dependent vesicular transport from early to late endosomes. J. Cell Biol. *123*, 1373–1387.

Aniento, F., Gu, F., Parton, R.G., and Gruenberg, J. (1996). An endosomal β COP is involved in the pH-dependent formation of transport vesicles destined for late endosomes. J. Cell Biol. *133*, 29–41.

Durrbach, A., Louvard, D., and Coudrier, E. (1996). Actin filaments facilitate two steps of endocytosis. J. Cell Sci. *109*, 457–465.

Emans, N., Gorvel, J.P., Walter, C., Gerke, V., Kellner, R., Griffiths, G., and Gruenberg, J. (1993). Annexin II is a major component of fusogenic endosomal vesicles. J. Cell Biol. *120*, 1357–1369.

Futter, C.E., Collinson, L.M., Backer, J.M., and Hopkins, C.R. (2001). Human VPS34 is required for internal vesicle formation within multivesicular endosomes. J. Cell Biol. *155*, 1251–1264.

Gerke, V., and Weber, K. (1984). Identity of p36K phosphorylated upon Rous sarcoma virus transformation with a protein purified from brush borders; calcium-dependent binding to non-erythroid spectrin and F-actin. EMBO J. *3*, 227–233.

Gruenberg, J. (2001). The endocytic pathway: a mosaic of domains. Nat. Rev. Mol. Cell Biol. *2*, 721–730.

Gruenberg, J., and Stenmark, H. (2004). The biogenesis of multivesicular endosomes. Nat. Rev. Mol. Cell Biol. *5*, 317–323.

Gruenberg, J., Griffiths, G., and Howell, K.E. (1989). Characterization of the early endosome and putative endocytic carrier vesicles in vivo and with an assay of vesicle fusion in vitro. J. Cell Biol. *108*, 1301–1316.

Harder, T., Kellner, R., Parton, R.G., and Gruenberg, J. (1997). Specific release of membrane-bound annexin II and cortical cytoskeletal elements by sequestration of membrane cholesterol. Mol. Biol. Cell *8*, 533–545.

Hayes, M.J., Merrifield, C.J., Shao, D., Ayala-Sanmartin, J., Schorey, C.D., Levine, T.P., Proust, J., Curran, J., Bailly, M., and Moss, S.E. (2004a). Annexin 2 binding to phosphatidylinositol 4,5-bisphosphate on endocytic vesicles is regulated by the stress response pathway. J. Biol. Chem. *279*, 14157–14164.

Hayes, M.J., Rescher, U., Gerke, V., and Moss, S.E. (2004b). Annexin-actin interactions. Traffic *5*, 571–576.

Hayes, M.J., Shao, D., Bailly, M., and Moss, S.E. (2006). Regulation of actin dynamics by annexin 2. EMBO J. *25*, 1816–1826.

Hayes, M.J., Shao, D.M., Grieve, A., Levine, T., Bailly, M., and Moss, S.E. (2008). Annexin A2 at the interface between F-actin and membranes enriched in phosphatidylinositol 4,5,-bisphosphate. Biochim. Biophys. Acta. Published online October 29, 2008. 10.1016/j.bbamcr.2008.10.007.

Jost, M., Zeuschner, D., Seemann, J., Weber, K., and Gerke, V. (1997). Identification and characterization of a novel type of annexin-membrane interaction: $Ca^{2+}$ is not required for the association of annexin II with early endosomes. J. Cell Sci. *110*, 221–228.

Kaksonen, M., Toret, C.P., and Drubin, D.G. (2006). Harnessing actin dynamics for clathrin-mediated endocytosis. Nat. Rev. Mol. Cell Biol. *7*, 404–414.

Kerkhoff, E., Simpson, J.C., Leberfinger, C.B., Otto, I.M., Doerks, T., Bork, P., Rapp, U.R., Raabe, T., and Pepperkok, R. (2001). The Spir actin organizers are involved in vesicle transport processes. Curr. Biol. *11*, 1963–1968.

Lloyd, T.E., Atkinson, R., Wu, M.N., Zhou, Y., Pennetta, G., and Bellen, H.J. (2002). Hrs regulates endosome membrane invagination and tyrosine kinase receptor signaling in *Drosophila*. Cell *108*, 261–269.

Mayor, S., and Pagano, R.E. (2007). Pathways of clathrin-independent endocytosis. Nat. Rev. Mol. Cell Biol. *8*, 603–612.

Mayran, N., Parton, R.G., and Gruenberg, J. (2003). Annexin II regulates multivesicular endosome biogenesis in the degradation pathway of animal cells. EMBO J. *22*, 3242–3253.

Merrifield, C.J., Rescher, U., Almers, W., Proust, J., Gerke, V., Sechi, A.S., and Moss, S.E. (2001). Annexin 2 has an essential role in actin-based macropinocytic rocketing. Curr. Biol. *11*, 1136–1141.

Morel, E., and Gruenberg, J. (2007). The p11/S100A10 light chain of Annexin A2 is dispensable for Annexin A2 association to endosomes and functions in endosomal transport. PLoS ONE *2*, e1118.

Morel, E., and Gruenberg, J. (2008). Annexin A2 binding to endosomes and functions in endosomal transport are regulated by tyrosine 23 phosphorylation. J. Biol. Chem. *284*, 1604–1611.

Nielsen, E., Severin, F., Backer, J.M., Hyman, A.A., and Zerial, M. (1999). Rab5 regulates motility of early endosomes on microtubules. Nat. Cell Biol. *1*, 376–382.

Oling, F., Bergsma-Schutter, W., and Brisson, A. (2001). Trimers, dimers of trimers, and trimers of trimers are common building blocks of annexin a5 two-dimensional crystals. J. Struct. Biol. *133*, 55–63.

Parton, R.G. (1994). Ultrastructural localization of gangliosides; GM1 is concentrated in caveolae. J. Histochem. Cytochem. *42*, 155–166.

Parton, R.G., Schrotz, P., Bucci, C., and Gruenberg, J. (1992). Plasticity of early endosomes. J. Cell Sci. *103*, 335–348.

Petiot, A., Faure, J., Stenmark, H., and Gruenberg, J. (2003). PI3P signaling regulates receptor sorting but not transport in the endosomal pathway. J. Cell Biol. *162*, 971–979.

Pollard, T.D. (2007). Regulation of actin filament assembly by Arp2/3 complex and formins. Annu. Rev. Biophys. Biomol. Struct. *36*, 451–477.

Pons, V., Luyet, P.-P., Morel, E., Abrami, L., van der Goot, F.G., Parton, R.G., and Gruenberg, J. (2008). Hrs and SNX3 functions in sorting and membrane invagination within multivesicular bodies. PLoS Biology *6*, e214.

Quinlan, M.E., Heuser, J.E., Kerkhoff, E., and Mullins, R.D. (2005). *Drosophila* Spire is an actin nucleation factor. Nature *433*, 382–388.

Raiborg, C., Bache, K.G., Gillooly, D.J., Madshus, I.H., Stang, E., and Stenmark, H. (2002). Hrs sorts ubiquitinated proteins into clathrin-coated microdomains of early endosomes. Nat. Cell Biol. *4*, 394–398.

Rebowski, G., Boczkowska, M., Hayes, D.B., Guo, L., Irving, T.C., and Dominguez, R. (2008). X-ray scattering study of actin polymerization nuclei assembled by tandem W domains. Proc. Natl. Acad. Sci. USA *105*, 10785–10790.

Rescher, U., and Gerke, V. (2004). Annexins–unique membrane binding proteins with diverse functions. J. Cell Sci. *117*, 2631–2639.

Salas-Cortes, L., Ye, F., Tenza, D., Wilhelm, C., Theos, A., Louvard, D., Raposo, G., and Coudrier, E. (2005). Myosin Ib modulates the morphology and the protein transport within multi-vesicular sorting endosomes. J. Cell Sci. *118*, 4823–4832.

Soldati, T., and Schliwa, M. (2006). Powering membrane traffic in endocytosis and recycling. Nat. Rev. Mol. Cell Biol. *7*, 897–908.

Taunton, J., Rowning, B.A., Coughlin, M.L., Wu, M., Moon, R.T., Mitchison, T.J., and Larabell, C.A. (2000). Actin-dependent propulsion of endosomes and lysosomes by recruitment of N-WASP. J. Cell Biol. *148*, 519–530.

Trajkovic, K., Hsu, C., Chiantia, S., Rajendran, L., Wenzel, D., Wieland, F., Schwille, P., Brugger, B., and Simons, M. (2008). Ceramide triggers budding of exosome vesicles into multivesicular endosomes. Science *319*, 1244–1247.

van der Goot, F.G., and Gruenberg, J. (2006). Intra-endosomal membrane traffic. Trends Cell Biol. *16*, 514–521.

van Genderen, I.L., van Meer, G., Slot, J.W., Geuze, H.J., and Voorhout, W.F. (1991). Subcellular localization of Forssman glycolipid in epithelial MDCK cells by immuno-electronmicroscopy after freeze-substitution. J. Cell Biol. *115*, 1009–1019.

Williams, R.L., and Urbe, S. (2007). The emerging shape of the ESCRT machinery. Nat. Rev. Mol. Cell Biol. *8*, 355–368.

Zobiack, N., Rescher, U., Ludwig, C., Zeuschner, D., and Gerke, V. (2003). The annexin 2/S100A10 complex controls the distribution of transferrin receptor-containing recycling endosomes. Mol. Biol. Cell *14*, 4896–4908.